Sensitivity of the MM5 mesoscale model to physical parameterizations for regional climate studies: Annual cycle

J. Fernández,[1] J. P. Montávez,[2] J. Sáenz,[3] J. F. González-Rouco,[4] and E. Zorita[1]

Received 6 September 2005; revised 18 August 2006; accepted 30 August 2006; published 16 February 2007.

[1] We present an analysis of the sensitivity to different physical parameterizations of a high-resolution simulation of the MM5 mesoscale model over the Iberian Peninsula. Several (16) 5-year runs of the MM5 model with varying parameterizations of microphysics, cumulus, planetary boundary layer and longwave radiation have been carried out. The results have been extensively compared with observational precipitation and surface temperature data. The parameterization uncertainty has also been compared with that related to the boundary conditions and the varying observational data sets. The annual cycles of precipitation and surface temperature are well reproduced. The summer season presents the largest deviations, with a 5 K cold bias in the southeast and noticeable precipitation errors over mountain areas. The cold bias seems to be related to the surface, probably because of the excessive moisture availability of the five-layer soil scheme used. No parameterization combination was found to perform best in simulating both precipitation and surface temperature in every season and subregion. The Kain-Fritsch cumulus scheme was found to produce unrealistically high summer precipitation. The longwave radiation parameterizations tested were found to have little impact on our target variables. Other factors, such as the choice of boundary conditions, have an impact on the results as large as the selection of parameterizations. The range of variability in the MM5 physics ensemble is of the same order of magnitude as the observational uncertainty, except in summer, when it is larger and probably related to the inaccuracy of the model to reproduce the summer precipitation over the area.

Citation: Fernández, J., J. P. Montávez, J. Sáenz, J. F. González-Rouco, and E. Zorita (2007), Sensitivity of the MM5 mesoscale model to physical parameterizations for regional climate studies: Annual cycle, *J. Geophys. Res.*, *112*, D04101, doi:10.1029/2005JD006649.

1. Introduction

[2] Estimations of future climate changes due to anthropogenic forcing are performed with the help of coupled atmosphere-ocean general circulation models (GCMs), which typically have a horizontal resolution of a few hundred kilometers. However, regional climate is greatly influenced by local features such as mountains or land use, which are not well represented in GCMs because of their coarse resolution. Downscaling techniques have been used in the last decades to overcome this problem in studies of climate change at regional scales [*Hewitson and Crane*, 1996].

[3] Downscaling techniques can be classified into two groups: simulations with regional climate models, and statistical/empirical models that link large-scale climate fields with local or regional climate variables [*Kidson and Thompson*, 1998; *Murphy*, 1999]. The use of a high-resolution regional climate model (RCM), nested into a GCM which provides the boundary conditions required by the RCM, has experienced enormous growth over the past decade. *Giorgi and Mearns* [1999] and *Wang et al.* [2004] offer recent reviews on the application of this particular approach, which has emerged in the wake of the increasing computational power and the availability of numerical model source code for the research community. RCMs provide a clear added value with respect to simulations with coarse resolution models [*Castro et al.*, 2005].

[4] Despite the higher resolution of RCMs, a number of physical processes that occur at subgrid scale have to be represented in the model by approximate parameterizations, which in many cases have a semiempirical basis. The range of validity of these parameterizations is not tightly constrained and may be valid only in certain regions or seasons. Since RCMs are usually applied to limited regions, of the order of a few thousand km^2, it may be assumed that a

[1]Institute for Coastal Research, GKSS Forschungszentrum, Geesthacht, Germany.
[2]Department of Physics, University of Murcia, Murcia, Spain.
[3]Department of Applied Physics II, University of the Basque Country, Bilbao, Spain.
[4]Departamento de Astrofísica y CC. de la Atmósfera, Universidad Complutense de Madrid, Madrid, Spain.

0148-0227/07/2005JD006649

single set of parameterizations should be valid or, at least, be as optimal as possible, for the whole domain of the simulations. Furthermore, parameterizations that may work well for a certain purpose, e.g., description of a severely convective event, may be clearly suboptimal for other applications at longer climatic timescales. For climatic applications, some might even fail, because during very long integrations they may not fulfill the necessary closure relationships.

[5] This assumption, however, is usually not systematically tested, probably because of the computational burden of performing a large number of relatively long simulations with different parameterizations. The question arises whether a single set of physical parameterizations can be used in regions with complex orography, and whether the same set is optimal throughout the annual cycle. We have investigated these questions by analyzing the performance of an RCM, namely the MM5 mesoscale model, in the Iberian Peninsula (IP), located in Southwestern Europe.

[6] The Fifth-Generation Penn State University/National Center for Atmospheric Research (PSU/NCAR) Mesoscale Model [*Grell et al.*, 1994], known as the MM5, is a nonhydrostatic, vertical sigma-coordinate model designed to simulate mesoscale atmospheric circulations. The most prominent features of the MM5 are multiple-nesting capability, availability of four-dimensional data assimilation (FDDA), and a large spectrum of physics options. The MM5 and some modified versions have been profusely used in regional climate studies [*Boo et al.*, 2004; *Liang et al.*, 2004a; *Oh et al.*, 2004; *Leung et al.*, 2004; *Leung and Wigmosta*, 1999; *Leung and Ghan*, 1999].

[7] The skill of an RCM simulation depends upon several factors such as the model itself [*Evans et al.*, 2005; *Christensen et al.*, 1997], physical options such as parameterizations [*Lynn et al.*, 2004; *Giorgi and Shields*, 1999], soil specification [*Pielke*, 2001], spatial configuration (horizontal and vertical resolutions, domain boundary location, ...) and nesting strategies [*Beck et al.*, 2004; *Denis et al.*, 2002, 2003; *Juang and Hong*, 2001; *Salvador et al.*, 1999], boundary conditions [*Denis et al.*, 2003; *Noguer et al.*, 1998; *Wu et al.*, 2005; *Warner et al.*, 1997], site and season [*Vidale et al.*, 2003], the use of data assimilation techniques (if any), etc. It seems there is no special model configuration that can produce better results.

[8] Several studies have dealt with the selection of different parameterizations using the MM5 [*Pan et al.*, 1996; *Wang and Seaman*, 1997; *Cassano et al.*, 2000; *Ferretti et al.*, 2000; *Warner and Hsu*, 2000; *Kotroni and Lagouvardos*, 2001; *Bright and Mullen*, 2002; *Cohen*, 2002; *Liang et al.*, 2004a]. Most of them focused on short-range weather events. The MM5 proved better at generating precipitation forecasts for the cold season using higher-resolution grids [*Wang and Seaman*, 1997]. A more detailed soil scheme was found to have little impact on precipitation, which is more influenced by the cumulus parameterization used [*Pan et al.*, 1996]. These conclusions were reached after analyzing short-range experiments and clear differences were also found at these timescales in the interaction amongst the schemes of the different nested domains in producing rainfall [*Warner and Hsu*, 2000]. However, it is not clear how these differences will affect the monthly timescales, as long-term (multiyear) sensitivity studies to multiple parameterization choice have not been carried out with this model. The closest approach to ours is the study by *Liang et al.* [2004a], which compared two different cumulus schemes during the summer seasons of a 21-year period over North America.

[9] The main goal of this paper is to quantitatively test the sensitivity of the MM5 to different combinations of the parameterizations available for its use as a downscaling tool for a midlatitude region of complex orography and land-sea contrast like the IP. More specifically, we intended to test whether a single parameterization set could yield acceptable results in this area when compared with observed precipitation and temperature station data. We restricted our analysis to the ability of the model to accurately represent the mean annual cycle of temperature and precipitation. This made it necessary to systematically test the set of parameterizations under different conditions and during a relatively long period. This contrasts with other previous studies, which had focused on operational weather forecasting, the analysis of episodes of meteorological interest [*Wang and Seaman*, 1997] or shorter time span integrations [*Christensen et al.*, 1997].

[10] The IP was the target region selected for this study since it offers some interesting features which stem from the interaction of the large-scale flow and a characteristic local/regional topography. It is located at Northern Hemisphere midlatitudes and its climate is strongly affected by the mean annual cycle of the location of the Atlantic storm track and its deviations. Because of the spatial gradient of the oceanic influence and the complex orography, the climate of the IP shows strong spatial gradients from the coast to the interior. The complex orography has a strong influence on the way baroclinic perturbations affect the local climate, as they shield regions from oceanic moisture advection, or on the appearance of summer thermal lows [*Millán et al.*, 1991]. From the point of view of a traditional climatic classification, the IP has long been recognized as a place where classifications change abruptly in small geographical scales [*Font-Tullot*, 2000]. The mean annual cycle of the interior and the east of the IP is characterized by a Mediterranean climate. Summers are warm and dry, with precipitation being mainly convective. Winters are cold and humid, and precipitation is mainly caused by large-scale synoptic systems. In the north and in the west the annual cycle is dominated by the Atlantic, with somewhat milder winters and more humid summers than in the interior.

[11] The analysis of the spatial and temporal variability of key climatic elements over the whole or some parts of the Iberian Peninsula has been the focus of several previous studies. Several authors have analyzed the interannual variability of precipitation over the whole area or some regions of coherent variability such as the Mediterranean or Cantabrian coasts [*Fernández-Mills*, 1995; *Fernández and Sáenz*, 2003; *Rodó et al.*, 1997; *Rodríguez-Fonseca and Serrano*, 2002; *Rodríguez-Puebla et al.*, 1998, 2001; *Romero et al.*, 1999; *Sáenz et al.*, 2001c; *Serrano et al.*, 1999; *Xoplaki et al.*, 2004]. Other works have analyzed the variability of temperature over the area, with some of these works analyzing also the physical causes behind this behavior [*Castro-Díez et al.*, 2002; *Oñate and Pou*, 1996; *Sáenz et al.*, 2001a, 2001b; *Xoplaki et al.*, 2003; *Pozo-Vázquez et al.*, 2001].

[12] Variability of precipitation in some parts of the IP is known to be closely connected to the large-scale North Atlantic atmospheric circulation, including the North Atlantic Oscillation [*von Storch et al.*, 1993; *Goodess and Palutikof*, 1998; *González-Rouco et al.*, 2000; *Trigo and Palutikof*, 1999, 2001; *Fernández and Sáenz*, 2003; *Sumner et al.*, 1995]. For this reason, precipitation in the IP has served as a successful example of statistical downscaling. However, less attention has been devoted to the field of dynamical downscaling. In long (multiyear) runs the IP appears only as a part of larger areas such as the Mediterranean region [*Noguer et al.*, 1998; *Vidale et al.*, 2003; *Moberg and Jones*, 2004]. There are comparisons of the skill of different RCMs in areas covering the IP, but they have only been run for short time periods [*Christensen et al.*, 1997].

[13] This work is structured as follows: section 2 briefly describes the data used in this study; the basic setup of the model and the different experiments performed are described in section 3; the results obtained are discussed in section 4; and concluding remarks are presented in section 5.

2. Data

[14] Initial and boundary conditions for the regional model were obtained from the National Centers for Environmental Prediction/National Center for Atmospheric Research (NCEP/NCAR) Reanalysis (hereinafter the NNR [*Kalnay et al.*, 1996]). The product interpolated to a 2.5° × 2.5° regular latitude-longitude resolution from the original T62 grid was used as initial and boundary conditions for the different regional model runs. NNR global fields were used with 6-hourly resolution for the period 1985–1989. The variables needed as boundary conditions for the MM5 model were temperature, wind, geopotential height and specific humidity at 17 pressure levels, surface pressure and sea surface temperature. The rest of the data sets described in this section were also obtained for the period 1985–1989.

[15] To test the dependence of the model results on the boundary conditions, the 40-year reanalysis of the European Centre for Medium Range Weather Forecasts (ERA40 from now on [*Uppala et al.*, 2005]) was also used to provide the initial and boundary conditions for the regional model in section 4.4. The original horizontal and vertical resolution of ERA40 was T159L60, much higher than that of NNR. For a proper comparison with the previous results, this data set was interpolated to the same 2.5° regular latitude-longitude grid used by the NNR.

[16] Observational data sets were used for comparison with the regional model output. Monthly average surface temperature data at 55 stations were obtained from the Spanish and Portuguese National Institutes of Meteorology (both referred to as INM in the following). In the case of precipitation, a monthly data set of 88 homogenized instrumental series [*González-Rouco et al.*, 2001] developed at the Universidad Complutense de Madrid (UCM) was used. Although the data set covered some areas beyond the IP (southern France and northern Africa), these sites were excluded from this study because the comparison with the model results was less reliable because of the relaxation of the model toward the outer domain (see below). The 5-year period running from 1985 to 1989 was chosen for the experiments because it was the period closest to the present for which this data set was available during the first stages of this study (it has now been extended to 1999).

[17] Monthly surface air temperature over sea was derived from the International Comprehensive Ocean-Atmosphere Data Set (ICOADS [*Worley et al.*, 2005]). This data set provided monthly statistics in a 1° × 1° grid using data from ship reports, buoys and other platforms.

[18] Additional monthly validation data sets were used in section 4.3 to compare the MM5 output with a high-resolution gridded data set and in section 4.5 to show the observational uncertainty in the observations of precipitation provided by different sources.

[19] The land gridded monthly database with 0.5° horizontal resolution [*New et al.*, 2000] developed at the Climatic Research Unit (CRU), University of East Anglia, was used as an alternative observational data set for precipitation and temperature in section 4.3. It is a product interpolated from rain gauges (precipitation) and thermometers (temperature).

[20] The precipitation data sets from the Climate Prediction Center (CPC) Merged Analysis of Precipitation (CMAP [*Xie and Arkin*, 1997]) and the Global Precipitation Climatology Project (GPCP [*Adler et al.*, 2003]) were used in section 4.5 along with the estimates from UCM, CRU and surface precipitation derived from ERA40. CMAP data are a monthly analysis product including gauge observations and satellite data. In this paper, the enhanced product merged with precipitation forecasts from NNR was used in its 2.5° × 2.5° version. GPCP data were also based on satellite estimates combined with gauges and, additionally, provided an estimation of the absolute random error arising from the sampling and the algorithms used.

[21] The analysis is therefore mainly focused on temperature and precipitation, the most commonly used variables in downscaling exercises, because they present distinct features, such as the strong spatial variability of precipitation and the relative smoothness of temperature. The physical causes for winter variability of these fields are also different: baroclinic eddies, in the case of precipitation [*Ulbrich et al.*, 1999], and enthalpy density transports by the stationary waves, in the case of temperature [*Sáenz et al.*, 2001a]. Therefore the analysis focuses on different aspects of the climate over the area. This does not mean that other fields will behave in the same way as precipitation and temperature do, but rainfall and temperature serve well as examples of variables of a different type. A more comprehensive analysis of a wide set of climatic elements is out of the scope of this paper.

3. MM5 Setup

3.1. Common Setup

[22] The spatial configuration of MM5 version 3.6 used to carry out our experiments consisted of two nested domains (see Figure 1). In the vertical, 24 full sigma levels were used. The top of the atmosphere was located at 100 mbar. Around 8 levels were located below 800 hPa. The coarser domain (D1) had an horizontal resolution of 135 km and the inner high-resolution domain (D2) was set to a grid spacing of 45 km. D2 fully covers the Iberian

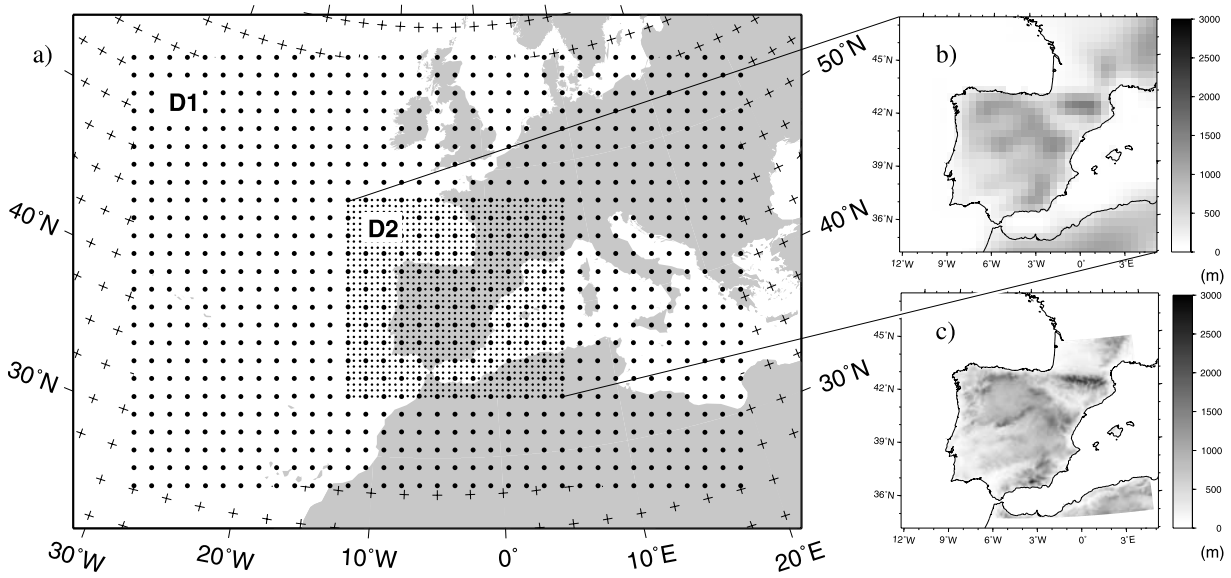

Figure 1. (a) Domains used in the simulations. Black crosses show the grid points of the NCEP/NCAR reanalysis, while the dots represent the grid points of the outer (D1) and high-resolution (D2) nested domains. (b) Orography of D2 as represented within the MM5. (c) Orography of D2 using the GTOPO30 database.

Peninsula even after excluding the 5 outermost grid points, which were affected by the relaxation to the outer domain (D1). Two-way nesting was used to feed the information from D2 back to the coarser domain. In D1 grid nudging was applied above the planetary boundary layer (PBL) by using Newtonian relaxation with the relaxation constants provided by default by the MM5 model. The NNR and ERA40 large-scale data were recorded every 6 hours and the boundary conditions for MM5 were obtained by linear interpolation at every model time step (ca. 7 min.).

[23] The solar constant and concentrations of greenhouse gases were kept constant during the integration period to the value prescribed in the model. As demonstrated by *Fernández* [2004], the results given by the model did not depend on initial values after one week; therefore a conservative spin-up of 2 months was applied at the beginning of the simulation, which was continuously integrated for a period of 5 years.

[24] The ground temperature was given by a five-layer soil model [*Dudhia*, 1996]. Whilst there was no explicit treatment of soil moisture, this quantity was prescribed according to soil characteristics and the season.

[25] Sea surface temperatures were taken from the skin temperature of the large-scale reanalyses. The amplitude of the daily skin temperature cycle in the MM5 drops quite realistically at the coastline, except for the area of the Strait of Gibraltar, which is considered land in the reanalyses. The summer amplitude in that area (6–8 K) is smaller than over land areas (8–14 K), although still not as small as in the surrounding open seas (<3 K).

[26] A further improvement of this study would be the use of a proper land surface model to account for interactive soil moisture content and the use of higher-resolution SST data. The latter, however, would only be useful for present climate studies, while the problem of the spatial crudeness of SSTs would remain for MM5 studies nested into coupled AOGCMs, which is one of the main final intentions when using RCMs. The use of a full land surface model is important for climate studies, although there are still systematic deficiencies that remain unsolved in the existing land surface models [*Zhu and Liang*, 2005].

3.2. Sensitivity Experiments

[27] The MM5 modeling system has several options for the different physical parameterizations (see Table 1). Several integrations (16) were performed by alternatively using two different parameterizations for four physical schemes: explicit moisture, cumulus convection, planetary boundary layer (PBL) and longwave radiation. In Table 1 the main options available in the MM5 v3.6 are listed. The four parameterizations used in this study are written in boldface. Notice that only a small amount of the possible combinations were covered in this study. The first two schemes for each parameterization were either nonrealistic or nonadequate for the spatial resolution we were using. For each one of the four physical parameterizations, a simple and a more complex option was selected for the sensitivity study. All the parameterizations selected have been commonly used in existing literature.

[28] Each model run, hereinafter referred to as an experiment, was performed with a single combination of parameterizations. Table 2 shows the 16 experiments carried out in this work and the computing time needed per simulated day. The experiment name is given by the combination of physical parameterizations in the order: **MCPR**, where **M** denotes Moisture Microphysics, **C** Cumulus, **P** PBL and **R** radiation schemes, identified by numbers, as given in Table 1.

[29] The first parameterization included in our sensitivity study was the explicit moisture scheme, which accounted for resolved precipitation. The schemes selected for the experiments were simple ice [*Dudhia*, 1989] and mixed phase [*Reisner et al.*, 1998]. The difference between these schemes

Table 1. List of the Main MM5 V3.6 Physical Schemes and Parameterizations Numbered as Internally Identified by the MM5 in the Configuration File[a]

Explicit Moisture	Cumulus	PBL	Radiation
Dry	none	none	none
Stable precipitation	Anthes-Kuo	bulk PBL	simple cooling
Warm rain	**Grell**	**Blackadar**	**cloud**
Simple ice	Arakawa-Schubert	Burk-Thompson	CCM2
Mixed-phase	Fritsch-Chappell	Eta	**RRTM**
Goddard	**Kain-Fritsch**	**MRF**	
	Betts-Miller	Gayno-Seaman	
	Kain-Fritsch 2	Pleim-Chang	

[a]Those used in the sensitivity study are in bold face.

is that the mixed phase scheme permits supercooled water and allows for slow melting of snow, while the simple ice uses a single array for cloud water (where the local temperature is above 0°C) and ice (in the entries where the local temperature is below the freezing point). Mixed phase cloud processes may play an important role in heavy rainfall events [*Wang and Yang*, 2003] and the existence of supercooled water in liquid phase instead of ice also implies different radiative properties.

[30] Another one of the main options which could potentially affect precipitation severely is the cumulus parameterization, which accounts for unresolved cloud formation. Depending on the grid resolution, convective clouds could be resolved by the explicit moisture scheme, but at the resolution used here (45 Km) it was necessary to parameterize cumulus formation. The feedback from these parameterizations to the larger-scale equations of the model is the profile of latent heat release and moistening caused by convection. The schemes used were the Grell (hereinafter GRCP [*Grell*, 1993]) and Kain-Fritsch (hereinafter KFCP [*Kain and Fritsch*, 1990]), both of which are mass flux schemes. There are two main differences between GRCP and KFCP. (1) In KFCP, the triggering depends on a temperature perturbation proportional to the grid-scale vertical velocity and the magnitude of the response depends on the convective available potential energy (CAPE), while in Grell, convection compensates the rate of change of destabilization due to advection. (2) KFCP remains active until the complete CAPE is removed whereas GRCP checks for its activation at every model time step. Thus once KFCP is activated, it may lead to longer-lasting clouds and more moist convection than GRCP. Even though the skill of a given parameterization may depend on the particular event, other cumulus parameterizations have proven to have less accuracy when compared with Grell and Kain-Fritsch in previous single-event studies, e.g., the Anthes-Kuo [*Pan et al.*, 1996; *Ferretti et al.*, 2000] or Betts-Miller schemes [*Cohen*, 2002]. The Kain-Fritsch scheme has shown good performance in several situations and regions [*Wang and Seaman*, 1997; *Kotroni and Lagouvardos*, 2001; *Cohen*, 2002]. In the study by *Ferretti et al.* [2000] in the Alpine region, the simple Grell scheme was better than the Kain-Fritsch scheme for certain events.

[31] Another important issue is the interaction between the atmosphere and the surface. The PBL schemes handle the latent and sensible heat fluxes into the atmosphere, the frictional effects with the surface and the strong subgrid-scale mixing which takes place in the lower levels because of these processes. In this case, the Blackadar [*Zhang and Anthes*, 1982] and MRF [*Hong and Pan*, 1996] schemes, both of which are complex, were used. These schemes are the best performing PBL parameterizations according to previous short-range studies [*Cassano et al.*, 2000; *Bright and Mullen*, 2002; *Berg and Zhong*, 2005]. Both are first-order nonlocal schemes, although MRF uses the counter gradient method and Blackadar the parcel method. The PBL scheme is likely to play a major role in the determination of surface temperature. Also, precipitation is affected since the PBL scheme heavily interacts with the cumulus scheme by providing the heat and moisture that determines the triggering of convective events.

[32] The last scheme selected for the sensitivity study was longwave radiation. Radiation calculations are quite costly and they are carried out every 30 model minute. The schemes used were the simplest ones taking into account the explicit cloud water calculated by the model: the "cloud" scheme [*Dudhia*, 1989], and an improved scheme, the Rapid Radiative Transfer Model (RRTM [*Mlawer et al.*,

Table 2. The 16 MM5 Experiments Performed[a]

Experiment ID	Microphysics	Cumulus	PBL	Radiation	CPU Time
4322	simple ice	Grell	Blackadar	cloud	177
4324	simple ice	Grell	Blackadar	RRTM	191
4352	simple ice	Grell	MRF	cloud	**149**
4354	simple ice	Grell	MRF	RRTM	**167**
4622	simple ice	Kain-Fritsch	Blackadar	cloud	182
4624	simple ice	Kain-Fritsch	Blackadar	RRTM	195
4652	simple ice	Kain-Fritsch	MRF	cloud	**152**
4654	simple ice	Kain-Fritsch	MRF	RRTM	**167**
5322	mixed phase	Grell	Blackadar	cloud	194
5324	mixed phase	Grell	Blackadar	RRTM	205
5352	mixed phase	Grell	MRF	cloud	168
5354	mixed phase	Grell	MRF	RRTM	186
5622	mixed phase	Kain-Fritsch	Blackadar	cloud	198
5624	mixed phase	Kain-Fritsch	Blackadar	RRTM	216
5652	mixed phase	Kain-Fritsch	MRF	cloud	171
5654	mixed phase	Kain-Fritsch	MRF	RRTM	184

[a]For each experiment the following are shown: the experiment identification number and the parameterizations used. The computing time (in wall-clock seconds per simulated day) required for each of the experiments is also shown (the four most economic experiments are in bold face).

1997]), for the longwave section of the spectrum. The cloud scheme only considers the interaction of radiation with water vapor and carbon dioxide whereas RRTM represents a detailed absorption spectrum taking into account water vapor, carbon dioxide, methane, nitrous oxide and ozone, all of which could be important in a climate change simulation. RRTM, which was used in combination with the previous cloud scheme for the shortwave, was included in this sensitivity study to check if it was worth the computational burden.

[33] All of these parameterizations interact with each other. The cumulus parameterization modifies the resolved cloud water/vapor content through detrainment, which in turn affects the microphysics. The microphysics parameterization determines the water content in the atmosphere and this affects the radiation. The radiation and PBL parameterizations interact through the surface fluxes given by the five-layer soil scheme. Additionally, the Grell cumulus scheme provides a cloud cover estimation which is directly used by the RRTM scheme. Also, the mixed phase scheme provides cloud ice which is used by the radiation scheme, while simple ice does not store ice independently and is thus not used as ice by the radiation scheme. Therefore there are some physical inconsistencies in the coupling between parameterizations in the sense that physical quantities obtained by some parameterizations (cloud ice, cloud cover, ...) are not systematically used by all the others. In this respect, efforts to improve the consistency between parameterizations in the MM5 have been undertaken [*Liang et al.*, 2004b], but there is still work to be done. Though this is out of the scope of this study, it is an important aspect for future studies to bear in mind.

4. Results

[34] To estimate the skill of the model and its parameterizations, monthly means were compared with the corresponding fields derived from observations. The degrees of freedom involved in this comparison include, apart from the 16 different parameterization combinations, the four seasons of the year, the different spatial locations and the different variables analyzed, namely, precipitation and temperature. The comparison of the model results with station data was done by bilinearly interpolating the model results to the station locations.

4.1. Precipitation

[35] Figure 2 (shading) shows the spatial distribution of the error corresponding to the experiment which has the smallest error in representing the annual cycle of precipitation for each season. The error for a season is computed as the root mean squared difference between the simulated and observed (according to UCM) monthly climatological means for the three months in that season. Errors range from 0 to 30 mm/month except for the stations at Grazalema (5°22′W, 36°46′N) and Penhas Douradas (7°33′W, 40°25′N), where the errors are greater than 100 mm/month during the autumn and winter seasons. These errors are probably due to the smoothed orography seen by the model, as can be appreciated in Figure 3. Figure 3 shows the differences between the real altitude of the stations and the altitude interpolated from the model orography. Thus positive differences correspond to stations in mountains truncated by the model and the negative ones represent stations in valleys and other low regions which were raised by the smoothed orography used in the simulations. The pattern of positive differences clearly matches the main error regions in winter and autumn. These errors are therefore likely to be reduced by using a grid of higher resolution in order to better capture the altitude of these stations.

[36] One of the main conclusions that can be drawn from Figure 2 is that no experiment shows the smallest error in every season and every area. Every experiment performs best (according to this seasonal RMS) in some location or season. The three experiments which more frequently performed the best are shown in Figure 2, together with the relative frequency that each parameterization performs the best, regardless of the combination in which this parameterization appears. In winter, the Grell cumulus and MRF PBL scheme show better results for southwestern IP and the northern coastline, whereas the Kain-Fritsch + Blackadar experiments perform better in the central and eastern IP. The results for the explicit moisture and longwave radiation schemes present less spatial agreement. In spring, the situation is similar, but with a clearer prevalence of the Kain-Fritsch cumulus scheme yielding the lowest error values. In summer, the situation reverses to a prevalence of the Grell cumulus scheme (in a season when the convective precipitation is a significant part of the total precipitation). The MRF scheme for the PBL is also preferred in summer. In autumn, no clear areas or general prevalence can be assigned.

[37] The seasons (spring and summer) and areas (southeastern) with less precipitation variability also show less absolute error in the estimation of the seasonal cycle. To remove this effect and also to show the sign of the errors, Figure 4 illustrates the seasonal average of the monthly relative error of the experiment with the lowest error for each season. In most of the regions, relative errors are within the −25% to 25% range.

[38] The most noticeable overestimation error occurred in the interior of the northern IP during winter and also along a narrow band running from north to south through the center of the IP in summer, with a value of 100%, but especially in southern coastal areas, where the values reached 280% (off the scale in the map) for the most accurate experiment.

[39] In order to show the spread among the different estimations and the systematic biases, Figure 5 presents the performance of each individual experiment for the area-averaged seasonal cycle in the northern interior IP (defined as 6–1°W, 40–43°N). According to Figure 4, in this region the precipitation is overestimated throughout the year. The main feature of the observed seasonal cycle is the anomalous low precipitation in March. March precipitation shows a decreasing trend in the last 4 decades [*Paredes et al.*, 2006]. This anomalous seasonal cycle is well reproduced by all of the experiments, despite the apparent positive bias. The spread among the experiments ranged between ∼10 and ∼35 mm/month throughout the year and is larger from April through August.

[40] Because of the positive bias present in all experiments, the experiment with the lowest departures is always the one which produces the smallest amount of rainfall

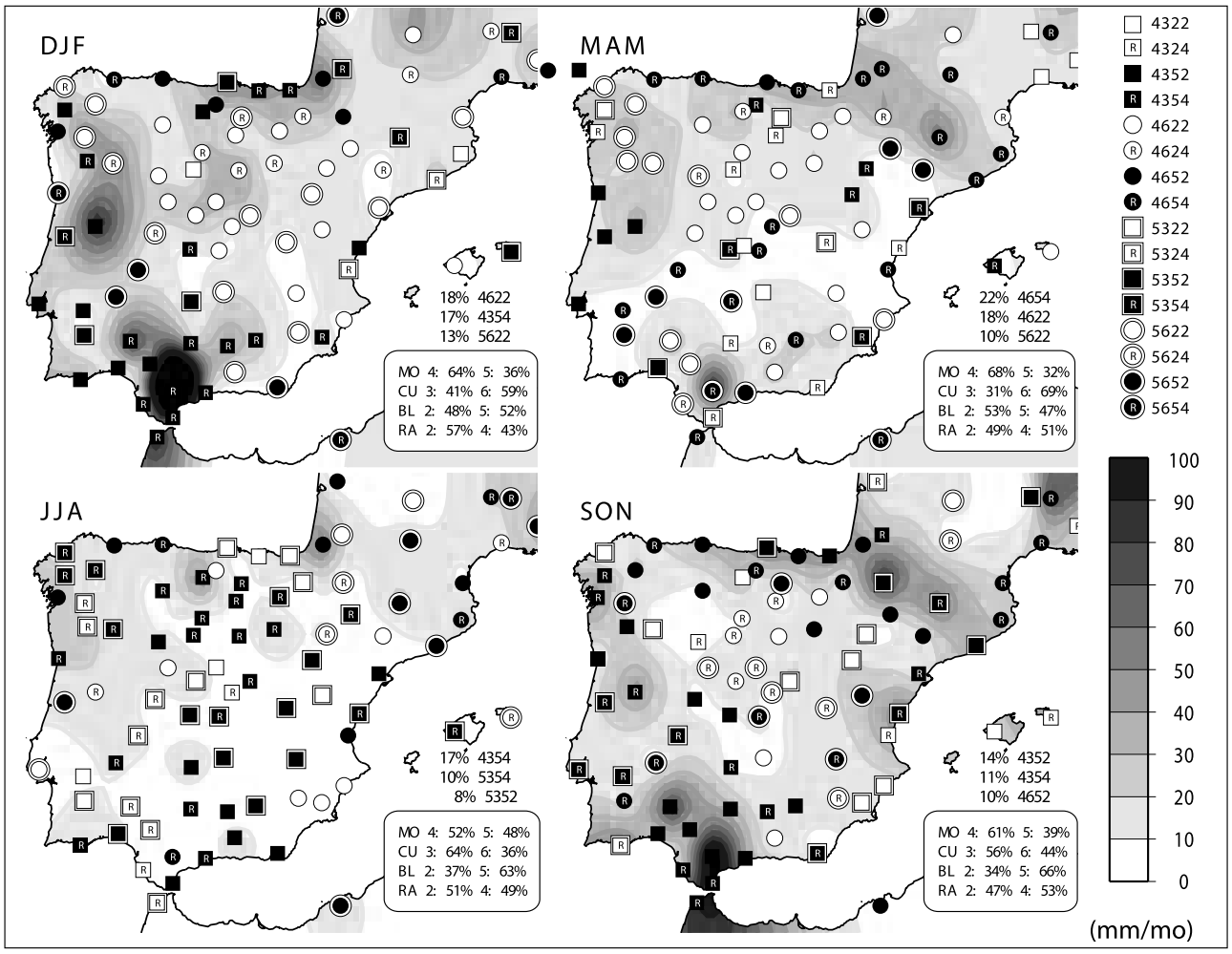

Figure 2. Optimal combination of parameterizations at each UCM station in terms of the RMSE of the simulated annual cycle of precipitation. The different symbols represent the experiments as follows: Double-line (simple) symbols represent mixed phase (simple ice) explicit moisture scheme. Squares (circles) are used for the Grell (Kain-Fritsch) cumulus scheme. Open (solid) symbols use the Blackadar (MRF) PBL scheme. Finally, those symbols showing an "R" include the RRTM longwave radiative scheme. The shading shows the RMS error. Also shown are the three experiments that outperform the others most often, in MCPR notation (see text and Table 2), and the percentage at which each parameterization performs best regardless of the combination in which the parameterization appears.

(except in September and October when the ensemble of experiments does not show any systematic bias). The optimal experiment in summer is, however, different from the best experiment in the rest of the year. To illustrate this fact more clearly, those experiments using the Kain-Fritsch parameterization are shown in black in Figure 5, while the rest are depicted in gray. The Kain-Fritsch cumulus scheme systematically produces more rainfall than the Grell scheme during summer, whereas it tends to produce less rainfall during the rest of the year. During summer months there is a clear gap between the experiments using the Kain-Fritsch scheme and the Grell scheme. This is in agreement with the different mechanisms producing rainfall in both schemes. The Grell scheme tests for possible convection at every time step, while Kain-Fritsch forces the release of all CAPE during a period of time once convection is triggered, making convective events last longer. This could explain the fact that KFCP overestimates precipitation during summer when the vertical instabilities are more likely to pass the triggering threshold than during the rest of the year. Most precipitation during summer months is due to small-scale convective events over the Iberian Peninsula [*Serrano et al.*, 1999].

[41] Figure 6 shows the partitioning of the precipitation in that produced by the explicit moisture scheme and the convective precipitation produced by the cumulus parameterization. For clarity, only the 8 experiments using the RRTM longwave radiation scheme are shown. The longwave radiation scheme produces only slight differences; therefore the other 8 experiments are very similar. The precipitation produced by the cumulus parameterization is responsible for the total precipitation differences in summer, with the KFCP producing around twice the precipitation of GRCP. In winter, the convective precipitation difference produced by both schemes is reduced, but KFCP still produces more precipitation. The cumulus parameterization

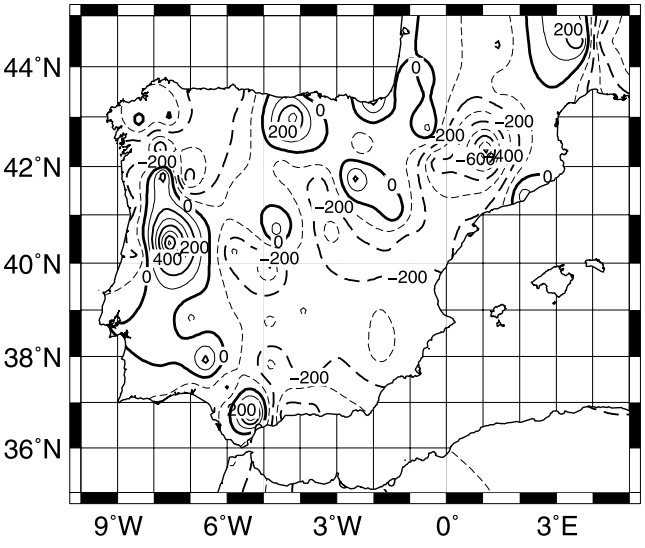

Figure 3. Orography anomalies at the UCM stations in meters. The model orography was interpolated to the UCM locations and subtracted from the station elevation data.

strongly affects the large-scale precipitation produced by the explicit moisture scheme. For instance, experiments 5354 and 5654 only differ in the cumulus scheme, but the mixed phase explicit moisture scheme produces less nonconvective precipitation when combined with the KFCP. The final effect on total rainfall is that KFCP produces more rainfall than GRCP in summer and less in winter, whereas the explicit moisture scheme plays a role in the partitioning of precipitation but not a sensible impact in the total amount. *Liang et al.* [2004b] already noticed the increased precipitation of KFCP with respect to GRCP over the United States and the inhibition produced by the latter in resolved precipitation. This effects are therefore not specific of our target area. However, the KFCP parameterization in the work by *Liang et al.* [2004b] was found beneficial in summer over the east coast of the U.S. where it helped in the correction of a dry bias of the model.

[42] In winter, the PBL scheme is the main parameterization producing differences in total precipitation. The MRF scheme systematically induces more rainfall than Blackadar. This was already found in previous short-range studies. For instance, *Wisse and Vilá-Guerau* [2004] attribute this effect to the enhanced atmospheric mixing of MRF compared to Blackadar, which induces more moisture to be efficiently transported to the free atmosphere, and thus makes more moisture available for precipitation.

4.2. Surface Temperature

[43] The surface temperature results (Figure 7) are more spatially homogeneous. Absolute errors are smaller in winter and the simple ice moisture, Kain-Fritsch cumulus, MRF PBL and RRTM schemes are preferred in most of the sites. In spring, the simpler cloud longwave radiation scheme outperforms the RRTM on the southwestern IP. In summer, the cloud scheme is better than the RRTM in most of the stations and mixed phase moisture + Grell cumulus prevail on coastal areas. Mixed phase moisture also prevails in several interior stations. In any case, the errors during summer reach values higher than 5° over the southeastern IP. In autumn, the preferred experiment is simple ice moisture, Kain-Fritsch cumulus, MRF PBL and cloud longwave radiation, except over the northwestern IP, where mixed phase moisture is preferred.

[44] The fact that the biases are smaller in winter, overtly independent of the parameterization, is probably due to the strong dependence of temperature on advection by the atmospheric circulation, i.e., on large-scale processes that are mostly prescribed by the boundary conditions. In summer, the local processes are more important and the parameterizations become more relevant in causing larger differences. This situation could be different when analyzing daily temperature ranges, where local cloudiness affecting the radiation balance in the shortwave and long-wave ranges may be more important than in the monthly means.

[45] Except for the winter season, when the errors are much lower, the spatial distribution of errors is stable from March through November, with increased intensity of the error pattern during summer. In this case, the temperature difference between the model and observations does not seem to be related to the altitude difference between model and reality (see Figure 3). The model underestimates the surface temperature throughout, except for a single station in Portugal, where the model terrain height is much lower than the real one and the temperature is thus overestimated.

[46] Figure 8a shows the annual cycle for the area with the highest error values. This area was selected as 4.5°W–0.3°E/36.5–42°N and contains 18 INM temperature stations. There is a systematic underestimation of the surface temperature throughout the year. The experiments better representing the seasonal cycle are just those simulating highest temperatures, which use the simple ice, Kain-Fritsch and MRF PBL schemes. The differences between both longwave radiation schemes are very small here (the maximum difference is 0.7 K in August between 5622 and 5624), but this is likely to be different in a climate change context, with increasing greenhouse gas concentrations. These gases are explicitly taken into account in the RRTM scheme, whereas the cloud scheme is only affected indirectly through the effects of these forcings on the circulation or moisture content of the GCM, which provides the boundary conditions. The high (in reference to the rest of experiments) temperatures in summer simulated by the combined simple ice, Kain-Fritsch and MRF PBL schemes (experiments labelled 465x) cannot be fully justified in terms of lower cloudiness than in other model runs. Though this seems the most obvious explanation, in fact, other combinations of parameterizations simulate higher downward shortwave radiation while giving rise to lower temperatures (Figure 8b). A full analysis of all the processes (divergence of net downward and upward radiative fluxes, or sensible and latent heat fluxes) in relation with key land processes (evaporation, emission and so on) was beyond the scope of this work. In fact, land processes were only scarcely considered in this study, since a full-featured land surface model was not used.

[47] We performed an additional experiment using the local Eta PBL scheme [*Janjić*, 1994] to discard the possibility that our selection of two nonlocal PBL schemes could be mixing excessively the surface air with the colder air aloft. The experiment used simple ice microphysics,

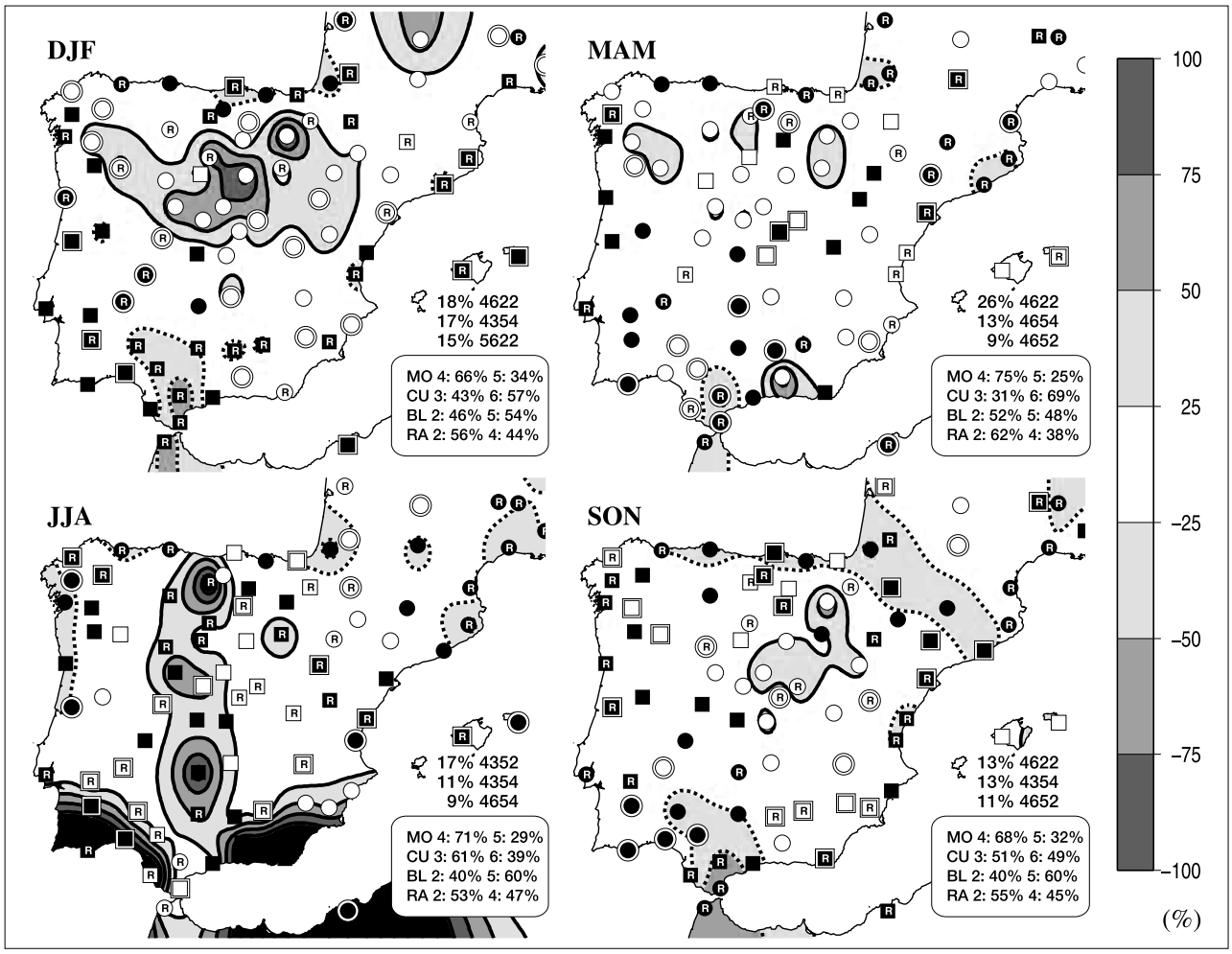

Figure 4. As in Figure 2 but using the relative error of the best experiment for each season. Dashed contours represent negative relative errors.

Kain-Fritsch cumulus, Eta PBL and the cloud radiation schemes. The results (not shown) yield an even colder bias, suggesting that the cold bias may arise from the processes at the surface and be more slowly mixed by the Eta scheme.

[48] A possible explanation for the cold bias obtained in summer over the southeastern interior regions could come from the lack of a proper land surface model to realistically represent soil moisture. Figure 9 shows this bias for July using experiment 4652. The bias was computed over land using CRU surface temperature data whereas over ocean the ICOADS 1° air temperature data was used. The strong cold bias was limited to land areas. Using the CRU surface data this bias reached −6.5°C. Over ocean the maximum bias was −3.7°C. The dryness of southeastern IP during summer lead to high surface temperatures. The model surface moisture availability was prescribed from seasonally varying standard values according to the land use. The standard moisture availability set by the model for the soil cover of southeastern IP is likely to provide an unrealistically high humidity content leading to lower surface temperatures than observed. There are two main USGS soil categories over this area, ''Dryland Cropland and Pasture'' and ''Cropland/Woodland Mosaic,'' which can be considered correct as an overall classification of the area. The moisture availability, and possibly other features, of these categories are, however, too high (0.3) for this area in summer. To overcome this effect, the surface moisture availability and other soil properties could be tuned over the area to better represent the land surface in this region. This tuning is obviously out of the scope of this paper.

[49] *Vidale et al.* [2003] included the IP in a similar RCM experiment using 3 different soil schemes. In spite of their sophisticated treatment of the soil moisture, their results showed only slightly weaker cold biases. Moreover, over the IP, the simplest soil model lead to the smallest summer surface temperature bias. On the other hand, our agreement of mean surface temperatures in winter was better than that obtained by *Vidale et al.* [2003]. The opposite effect was reported by *Christensen et al.* [1997] in a comparison of multiple RCMs including LSM. The LSM showed a tendency to dry out the soil in summer and this effect lead to an unrealistic increase of the surface temperatures over most of southern Europe.

4.3. Distribution of Precipitation and Temperature

[50] The CRU data set provided us with regularly gridded monthly data at a resolution similar to that of the MM5 experiments performed for this study. Even though its

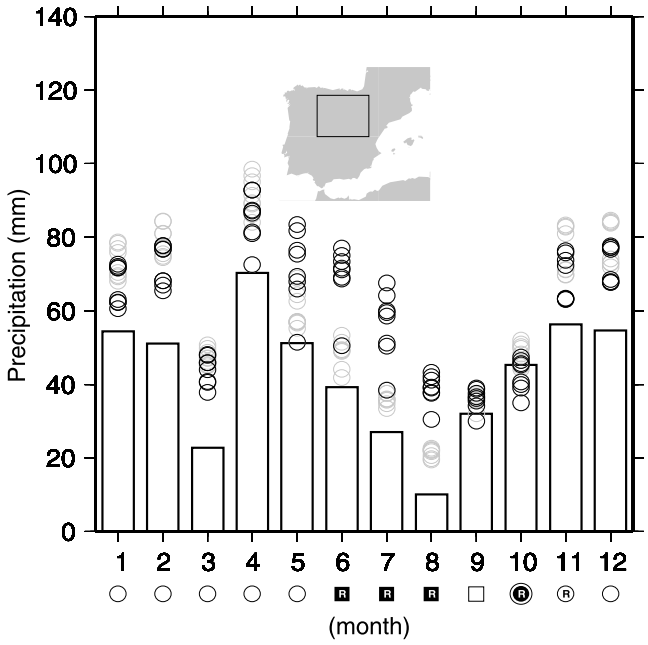

Figure 5. Area-averaged annual cycle of precipitation for the interior of northern IP (6–1°W, 40–43°N). For each month, the bar shows the observed precipitation according to the UCM data set and the circles the estimates derived from the 16 experiments. The best experiment for each month is also shown with the symbols defined in Figure 2. Solid circles represent the experiments using Kain-Fritsch, and shaded circles represent those using Grell.

accuracy to represent the interannual variability over our target area could be compromised because of the sparse original observed data [*Fernández and Sáenz*, 2003], the climatological mean was obtained through an altitude-dependent algorithm [*New et al.*, 1999]. A better spatial distribution of the variables should be expected from this data set than from a simple interpolation of the station data used in previous sections onto a regular grid.

[51] For the months of January and July, the experiments which performed best in precipitation according to Figure 2 were compared with the monthly climatologies from CRU for these months (Figure 10). To illustrate the observational error, the results for the UCM station data are also shown. Since the CRU data set is an spatially averaged product, it is also unable to capture the higher values of precipitation produced in some mountain stations. This behavior is evident in January in Grazalema (where the UCM precipitation is 428 mm/month, out of the scale in Figure 10 and shown in white), Penhas Douradas, and some stations in the Pyrenees. In July, both observational data sets mostly agree except for a single station in the Pyrenees.

[52] The simulation selected for January (Figure 10b) was simple ice microphysics, Kain-Fritsch CP, Blackadar PBL and cloud radiation (4622), which should give better results in the central and eastern IP according to Figure 2a. The mean precipitation pattern over land closely resembles that of CRU except over the southwestern IP where lower than observed precipitation was simulated. The behavior in this region improved in an experiment with Grell cumulus and MRF PBL, e.g., 4352 (not shown).

[53] In summer, the experiment using simple ice microphysics, Grell CP, MRF PBL and RRTM longwave radiation (4354) is shown (Figure 10d). The precipitation was, in general, higher than observed and a high spatial variability was produced by the model over the mountain regions in northern IP.

[54] The results for temperature (Figure 11) are much better than for precipitation. The experiments using simple ice microphysics, Kain-Fritsch CP and Blackadar PBL were used. RRTM longwave radiation scheme was used in winter

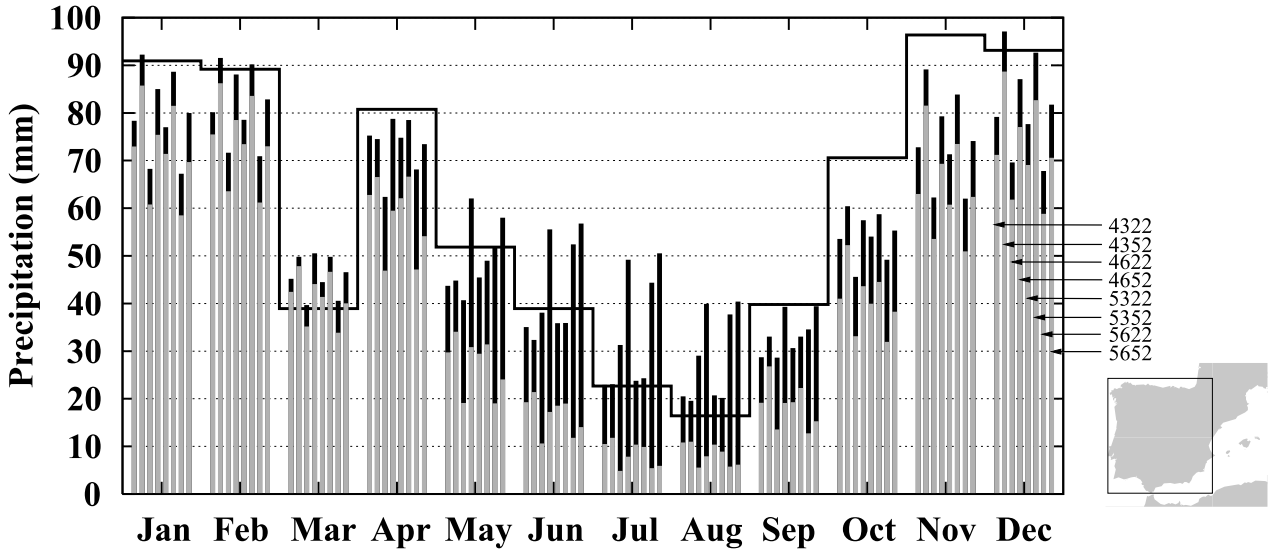

Figure 6. Area-averaged annual cycle of precipitation for the whole IP. The line shows the observed precipitation according to UCM and the full length of the bars shows the estimates derived from the 8 MM5 experiments using the RRTM longwave radiation scheme. The lower shaded part of each bar shows the nonconvective precipitation, and the solid part shows the convective one.

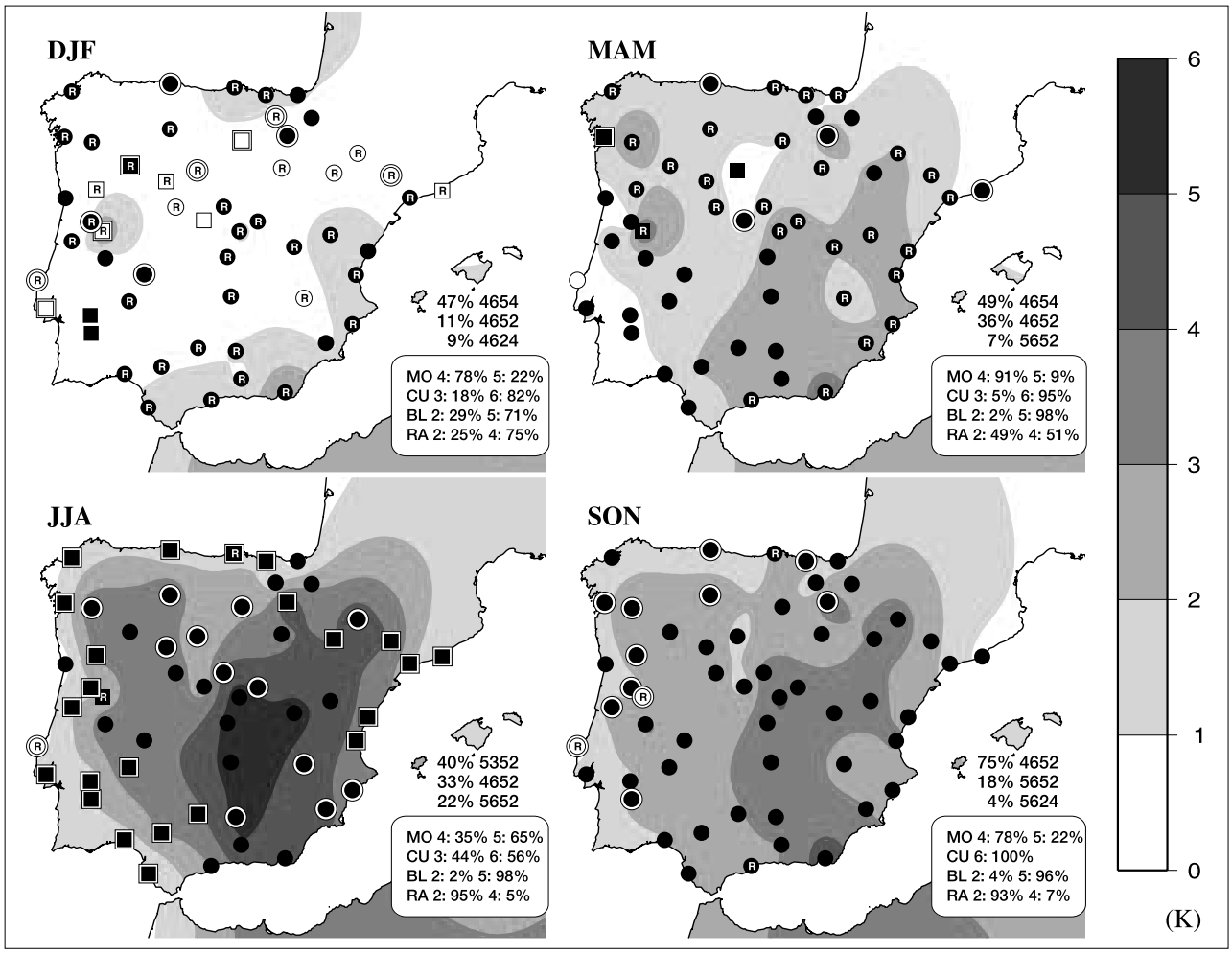

Figure 7. As in Figure 2 but for 2 m temperature.

and cloud scheme in summer. The spatial pattern in January is very well captured in shape and intensity. In summer, the pattern is also well captured (this was expected, since it is closely related to the orography), but it is systematically shifted (around 5°C in the southern IP and lower toward the north) to cooler temperatures than observed. There are regions of error compensation, e.g., the Pyrenees, where the general cooling effect is compensated by the warmer temperatures because of the smoothed model orography.

4.4. ERA40 Boundary Conditions

[55] The previous results systematically show the sensitivity of the results of a long MM5 integration to a subset of the huge amount of possible experiments. They illustrate the level of uncertainty inherent in the choice of model parameterization. The number of possible experiments becomes infinite when the possibility of changing the adjustable continuous parameters within each parameterization is taken into account (for instance, the values of precipitation efficiency or the cloud radius in the KFCP may be changed in a continuous way). In an ideal modeling approach it should be possible to select the optimal parameterizations and adjustable parameters in such a way that the results best fit the observations for every considered variable and at each location, season and timescale considered. In practical terms, however, a reasonable fit of every one of the mentioned degrees of freedom with a single experiment is unlikely to be reached. For instance, in the previous section it was shown that the best choice of parameterizations for surface temperature was not appropriate for precipitation.

[56] Another fact that should be considered is the uncertainty of the ''real'' (observed) large-scale atmospheric and surface conditions driving the RCM. The regional model can only be fitted to the observations to the extent that the driving large-scale conditions correspond to the observed large-scale fields. This section considers this source of uncertainty by comparing the results from a single previous experiment with its counterpart using a different set of boundary conditions (i.e., when embedded in a different ''real'' large-scale forcing).

[57] For this purpose, the European Centre for Medium-Range Weather Forecasts (ECMWF) Reanalysis (ERA40) was considered as the boundary condition. The experiment selected was the one with simple ice microphysics, Grell CP, MRF PBL and RRTM longwave radiation (4354) schemes. Figure 12 shows the annual cycle of precipitation in the interior of the IP, as in Figure 5, but includes this new experiment. Boundary conditions play an important role in determining local precipitation. The main effect of the ERA40 boundary conditions was increased precipitation

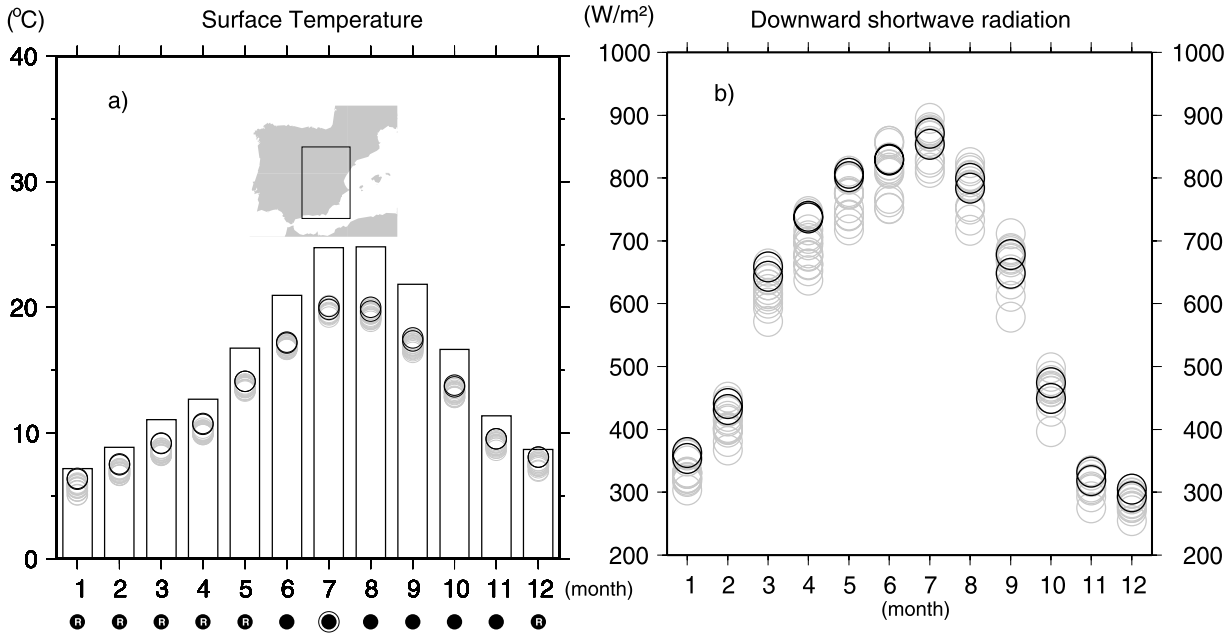

Figure 8. Area averaged annual cycle of (a) 2 m temperature and (b) downward shortwave radiation at 12Z over southeastern IP. Each circle represents the estimates derived from the 16 MM5 experiments. Experiments using the combination of simple ice, Kain-Fritsch and MRF schemes are shown as solid and the rest are shown as gray. In Figure 8a, for each month, the bar shows the observed temperature from INM. The experiment closest to the observed value is shown for each month with the symbols defined in Figure 2.

(except in November). This was also true for other regions (not shown). In this particular case, where precipitation was already overestimated, the NNR boundary conditions performed better than ERA40. Of course, in other regions/months where the precipitation was underestimated this effect reduced the error.

[58] This shows that an overall bias in the RCM simulation may be brought about by the data set used as boundary conditions, and this has to be taken into account when estimating the skill of the RCM. On the other hand, the systematic bias could be correctable by statistical means.

4.5. Observational Uncertainty

[59] As a final uncertainty measure, this section compares the different estimates of the local variables derived from different observational data sets. Up to this point, the precipitation data collected at the UCM was considered as the reference estimate of local precipitation. Data sets from

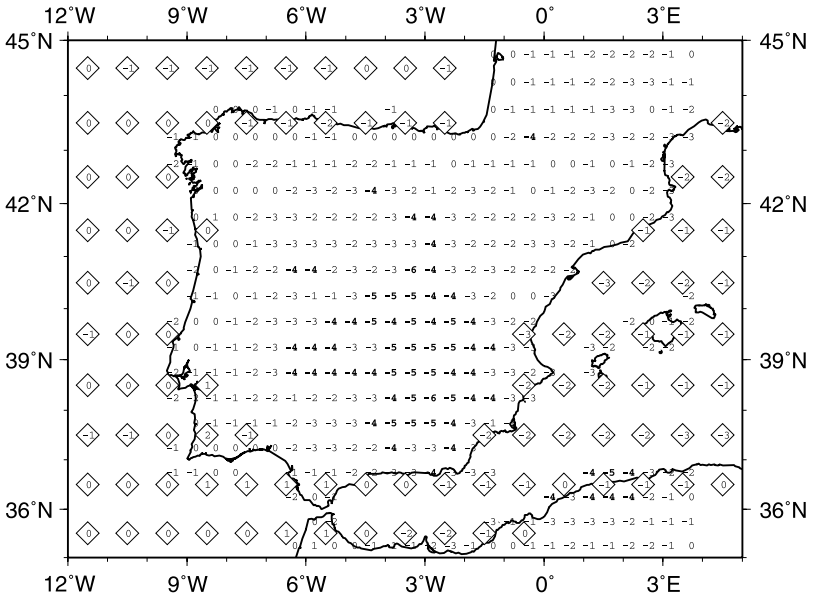

Figure 9. Surface temperature bias of July climatology according to experiment 4652. Grid points over land show the bias from CRU data and those over sea the bias from ICOADS data.

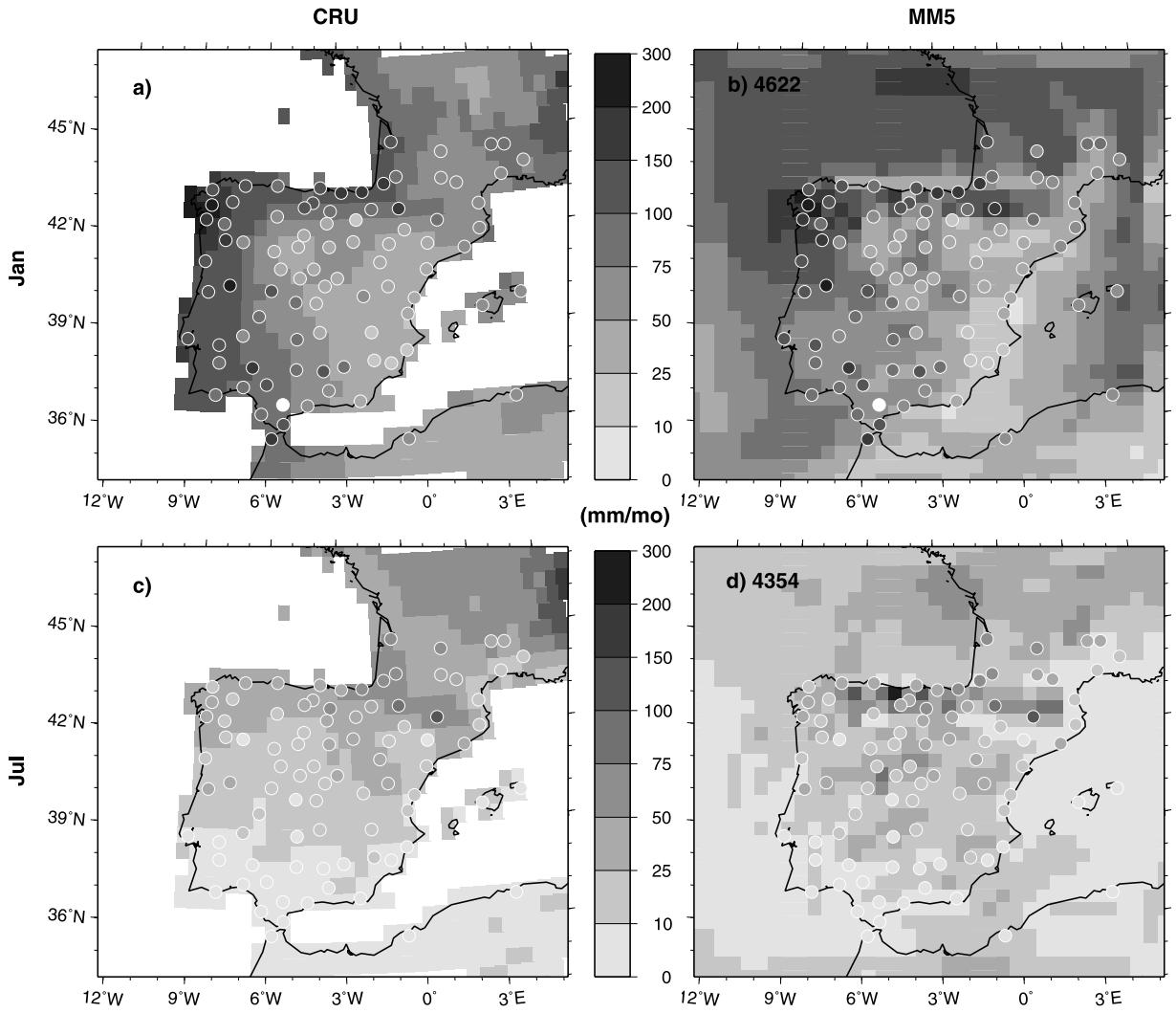

Figure 10. Monthly precipitation climatology for (a and b) January and (c and d) July according to CRU (Figures 10a and 10c) and MM5 (Figures 10b and 10d). The value according to the UCM stations is shown in the superposed circles.

other sources are available for the region, although these are quality controlled on a global scale and not specifically for our area of interest. Also, the number of observation sites is higher than, for instance, the high-resolution CRU data set, which is based on fewer stations than the UCM provides.

[60] The annual cycle of precipitation derived from NNR, CMAP, ERA40, CRU and GPCP is shown in Figure 13, along with the UCM estimate and the 16 MM5 experiments performed in this study. Note that in Figure 13, the average rainfall for the whole area is shown, instead of the average of the subset of the stations with winter positive bias, as in Figure 5. To avoid possible biases due to the irregular location of the UCM stations, all data sets were bilinearly interpolated to the UCM stations prior to the average. The estimation of the error provided by the GPCP product is also shown as an additional measure of the uncertainty in the observational estimates.

[61] The NNR estimate has been included as a measure of the added value of dynamical downscaling. It is the precipitation as produced by the NCEP global model based on circulation and moisture fields which most closely resemble those observed in the atmosphere (through data assimilation). The NNR strongly underestimates the October–February precipitation. The other reanalysis product, ERA40, shows a very similar behavior in this season. On the other hand, the precipitation during May–July is overestimated and, in this case, ERA40 shows an opposite behavior. The same circulation and moisture fields were fed into our MM5 experiments. The MM5 results for precipitation lie closer to the purely observational data sets.

[62] The coarse resolution of these observational data sets (except CRU) could still lead to an underestimation of the precipitation due to the smoothing inherent in the spatial grid point average, but this does not seem to be the case except for the ERA40 data, which produces low precipitation throughout the year. Precipitation in ERA40 is a model product and thus is affected by the coarse model orography which dynamically induces less precipitation. The full-resolution ERA40 precipitation was also used to check whether the interpolation to 2.5° had played a relevant role

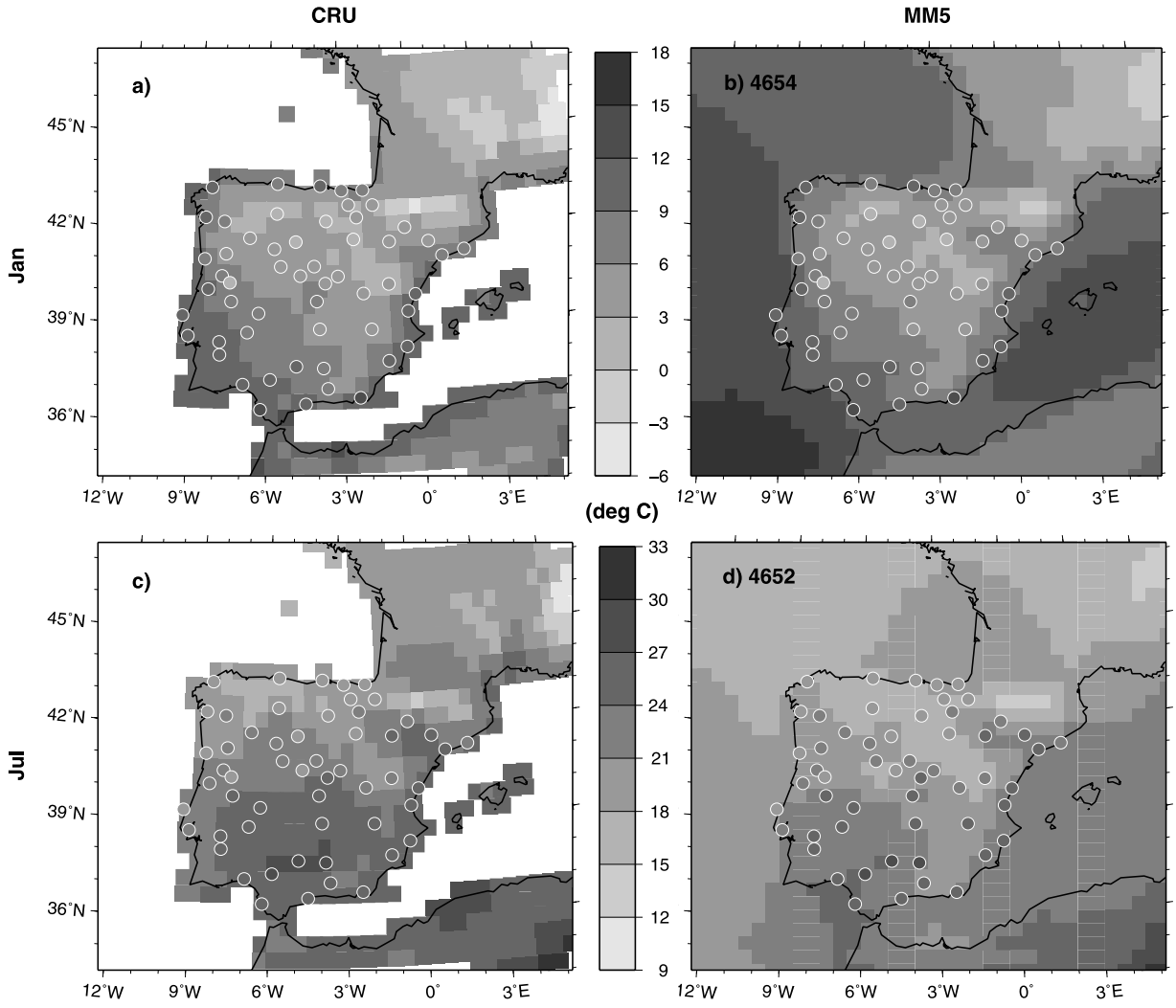

Figure 11. As in Figure 10 but for 2 m temperature.

in this underestimation, but the results (not shown) were nearly identical. The data set more closely following our previous reference data set is the GPCP, whose estimated random error embraces the CMAP, CRU and UCM estimates in every month.

[63] In every season except in summer the spread among the different observational data sets is larger than the spread of the MM5 ensemble. These results reinforce the ideas stated in previous sections, indicating that the best parameterization combination cannot generally be set. Furthermore, it illustrates that identification of the best parameterization combination is burdened by uncertainty in the target variable. These results also put the errors of the RCM into the framework of observational uncertainty. Even though the spread among the experiments was relatively high when compared with a single reference data set, the performance of the simulations clearly improved when compared with the ensemble of observations. Moreover, the uncertainty of the MM5 ensemble is of the same order of magnitude as the observational uncertainty when excluding the direct output from ERA40, which was already stated as unrealistic.

[64] In summer, the spread of the MM5 ensemble is larger than the observational spread and furthermore there is a clearer separation between the observational and simulated ensembles. This indicates that the overestimation of precipitation in these months is a real deficiency of the model and not the result of the uncertainty.

5. Conclusions

[65] A set of 16 dynamical downscaling experiments were performed using the MM5 modeling system in which two possible choices for four parameterization schemes (the explicit moisture, cumulus, PBL and longwave radiation) were systematically explored. The experiments were 5-year runs for the period 1985–1989 over the Iberian Peninsula nested into the NNR large-scale data.

[66] The study focused only on the annual cycle of precipitation and temperature, and the simulations were compared with several observational data sets. Additional nonsystematic tests were carried out to compare the parameterization uncertainty with the boundary condition and observational uncertainties.

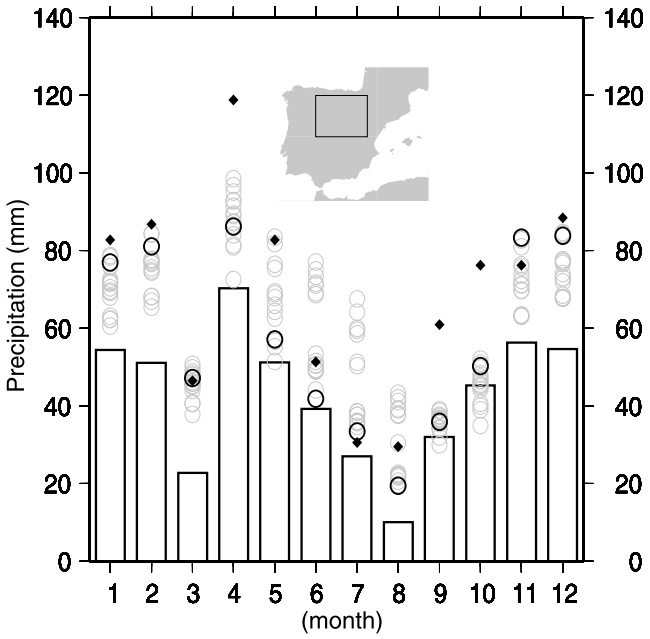

Figure 12. Area-averaged annual cycle of precipitation over northern interior IP according to UCM stations (bars) and the 16 MM5 experiments using NNR boundary conditions (shaded circles). Experiment 4354 is highlighted in black. Diamonds show this experiment using ERA40 boundary conditions.

[67] Several conclusions can be reached on the overall performance of the MM5 in long-term integrations over the IP. The area-average annual cycle over different regions is, in general, well captured. The anomalous seasonal cycle of precipitation in the modelled period during spring is reproduced in every experiment. Some biases are also evident, though. Precipitation is overestimated over the northern interior IP and temperature is underestimated over the whole area and throughout the year, with increased negative bias over the southeast in summer, where values of more than -5°C are reached. The spatial distribution of the monthly climatology of precipitation and temperature is also generally well captured. The main problems appear in summer, when excessive precipitation is produced over mountain regions and a cold bias develops in the southern part. The smoothed orography represented by the model was found to have a larger impact on precipitation during winter than in summer.

[68] The cold bias could be linked to the simple soil treatment used, with seasonally prescribed soil water. Further insight on this bias should be gained by performing a sensitivity test to better select the soil characteristics or by adding a more sophisticated land surface model. This bias is a feature common to every parameterization tested, so it is out of the scope of this sensitivity study.

[69] Concerning the different parameterizations under study, not all of them have the same impact on the variables tested, at least for this area:

[70] 1. For the explicit moisture scheme, none of the schemes analyzed was found to perform best for any particular region or season. For precipitation, this scheme was found to be responsible for the increase in winter precipitation when any one of the schemes tested was combined with the Grell cumulus scheme.

[71] 2. For the cumulus scheme, precipitation is most sensitive to the cumulus parameterization. Kain-Fritsch produces in general more convective precipitation, especially in summer, when it is unrealistically high. The Grell scheme induces more nonconvective precipitation in winter, leading to a better performance of the Kain-Fritsch scheme in this season. For temperature, the Kain-Fritsch scheme is usually better.

[72] 3. For the PBL scheme, precipitation was most sensitive to the PBL scheme during winter. The Blackadar scheme produces less winter rainfall than MRF regardless of the explicit moisture or cumulus schemes they were combined with. For temperature, MRF simulated higher temperatures and this lead to a better fit with the observations.

[73] 4. For the longwave radiation scheme, even though the selection of this parameterization can be a major computational burden, the results of the simple cloud scheme are very similar to those obtained using the detailed RRTM scheme. Other studies [*Liang et al.*, 2004b], however, found the radiation parameterization essential for precipitation. Supplementary results from a single experiment using the CCM2 radiation scheme (not shown) also suggest a beneficial effect, since the excessive summer precipitation was partially reduced. Thus the present study still requires a larger ensemble of combinations for a better assessment of the uncertainty in the selection of the physics schemes.

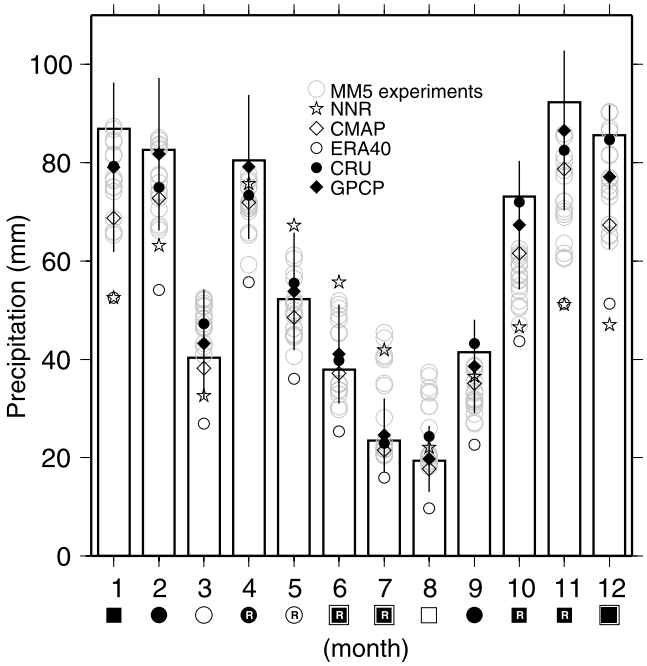

Figure 13. Area-averaged annual cycle of precipitation according to UCM stations (bars), the 16 MM5 experiments, CMAP, ERA40 2.5, GPCP (with error estimates) and the CRU 0.5 gridded data. Every data set is first bilinearly interpolated to the UCM stations and then averaged to avoid errors arising from the different coverage density of the UCM stations.

[74] The question of which are the best parameterizations for this area is thus not a simple matter. The question should even be changed to: Do the best parameterizations for this area exist? In most cases, systematic biases determine which parameterization set matches the observations better. After the correction of these biases, the parameterization with the best performance could change. Moreover, this study is only focuses on monthly climatologies. The skill of the different parameterizations in reproducing the interannual variability will be analyzed in a forthcoming study, and some of the parameterizations identified as the best at simulating the annual cycle may not be optimal for the variability in the same subregion, season and variable.

[75] In any case, some guidance for the selection of the best parameterizations can be extracted from this study to achieve a better simulation of the monthly seasonal cycle for a particular variable, season and, in most cases, valid only for certain subregions. The best parameterization is, however, dependent of the subregion/season/variable. A feasible adaptation of the model for a better fit could be a simulation in which the physical parameterizations change according to the season, restricting the target area to a smaller and more climatically homogeneous region.

[76] Another computationally more costly approach, could be a multiparameterization ensemble, which could be more meaningful than deterministic integrations. Figure 13 shows that the spread of the MM5 ensemble is consistent with the observational uncertainty. This ensemble could also include other uncertainties, such as those arising from the boundary conditions, which were shown to have an impact on surface variables comparable to the parameterizations tested systematically.

[77] The MM5 is therefore a valid tool to estimate the monthly climatology of surface variables, such as precipitation or temperature, which are highly dependent on regional features. Some biases are, however, apparent. For the application of the model results this bias should be corrected by statistical means, otherwise anomalies should be used for further analysis.

[78] The comparison of multiple observational data sets with the simulated results made it evident that the use of a single observational data set to validate the model results could be misleading in data scarce regions. The fact that not only the model, but also the observations, contain errors must always be taken into account. In the present study, the winter differences due to the use of different physical parameterizations were of the same order of magnitude as the differences between commonly used observational data sets. In summer, this comparison helps to reveal a likely model bias.

[79] As a final cautionary remark on the applicability of these conclusions, it is worth mentioning that the results could be highly dependent on the region and could also suffer from sampling uncertainty. Some results, however, are likely to be independent of the period selected for the analysis (e.g., the increased precipitation of KFCP in summer or the widespread underestimation of temperature). Also, the range of parameterizations tested in this study was limited by computational capabilities, and other schemes (see Table 1) or the parameterization of other physical processes could affect the analyzed variables in different ways. The inability of identifying a single optimal combination of parameterizations valid for every subregion, season and variable is, however, evident from this study.

[80] **Acknowledgments.** This study was financially supported by projects REN2002-04584-C04-01-CLI, REN-2002-04584-C04-04-CLI, CGL2005-06966-C07-04/CLI and CGL2005-06966-C07-05/CLI of the Spanish Ministry of Science and Technology. Jesús Fernández received support from the Department of Education, Universities and Research of the Basque Autonomous Government through grant BFI04.52. J. Sáenz received support by the research groups' support program, project 9/UPV 00060.310-15343/2003, University of the Basque Country. The gridded precipitation and temperature data were supplied by the Climate Impacts LINK Project (UK Department of the Environment Contract EPG 1/1/16) on behalf of the Climatic Research Unit, University of East Anglia. The boundary conditions were downloaded from the NCEP/NCAR Web server. The National Institutes of Meteorology of Spain and Portugal provided access to daily records of temperature and precipitation at several sites. Other surface and boundary data were provided by the MARS system of the ECMWF. The authors thank the Pennsylvania State University/National Center for Atmospheric Research numerical model home page for making the MM5 model publicly available. Authors made extensive use of the Generic Mapping Tools software [*Wessel and Smith*, 1991]. GTOPO30 topography data are distributed by the Land Processes Distributed Active Archive Center (LP DAAC), located at the U.S. Geological Survey's EROS Data Center http://LPDAAC.usgs.gov. We appreciate the comments on the manuscript made by Jimy Dudhia. The comments by three anonymous reviewers have also improved the final version of this manuscript.

References

Adler, R. F., et al. (2003), The version 2 global precipitation climatology project (GPCP) monthly precipitation analysis (1979–present), *J. Hydrometeorol.*, *4*, 1147–1167.

Beck, A., B. Ahrens, and K. Stadlbacher (2004), Impact of nesting strategies in dynamical downscaling of reanalysis data, *Geophys. Res. Lett.*, *31*, L19101, doi:10.1029/2004GL020115.

Berg, L. K., and S. Zhong (2005), Sensitivity of MM5-simulated boundary layer characteristics to turbulence parameterizations, *J. Appl. Meteorol.*, *44*(9), 1467–1483.

Boo, K., W. Kwon, J. Oh, and H. Baek (2004), Response of global warming on regional climate change over Korea: An experiment with the MM5 model, *Geophys. Res. Lett.*, *31*, L21206, doi:10.1029/2004GL021171.

Bright, D. R., and S. L. Mullen (2002), The sensitivity of the numerical simulation of the southwest monsoon boundary layer to the choice of PBL turbulence parameterization in MM5, *Weather Forecasting*, *17*, 99–114.

Cassano, J. J., T. R. Parish, and J. C. King (2000), Evaluation of turbulent surface flux parameterizations for the stable surface layer over Halley, Antartica, *Mon. Weather Rev.*, *129*, 26–46.

Castro, C. L., R. A. Pielke Sr., and G. Leoncini (2005), Dynamical downscaling: Assessment of value retained and added using the Regional Atmospheric Modeling System (RAMS), *J. Geophys. Res.*, *110*, D05108, doi:10.1029/2004JD004721.

Castro-Díez, Y., D. Pozo-Vázquez, F. S. Rodrigo, and M. J. Esteban-Parra (2002), NAO and temperature variability in southern Europe, *Geophys. Res. Lett.*, *29*(8), 1160, doi:10.1029/2001GL014042.

Christensen, J. H., B. Machenhauer, R. G. Jones, C. Schär, P. M. Ruti, M. Castro, and G. Visconti (1997), Validation of present-day regional climate simulations over Europe: LAM simulations with observed boundary conditions, *Clim. Dyn.*, *13*, 489–506.

Cohen, C. (2002), A comparison of cumulus parameterizations in idealized sea-breeze simulations, *Mon. Weather Rev.*, *130*, 2554–2571.

Denis, B., R. Laprise, D. Caya, and J. Côté (2002), Downscaling ability of one-way-nested regional climate models: The Big-Brother experiment, *Clim. Dyn.*, *18*, 627–646.

Denis, B., R. Laprise, and D. Caya (2003), Sensitivity of a regional climate model to the resolution of the lateral boundary conditions, *Clim. Dyn.*, *20*(2–3), 107–126.

Dudhia, J. (1989), Numerical study of convection observed during the winter monsoon experiment using a mesoscale two-dimensional model, *J. Atmos. Sci.*, *46*, 3077–3107.

Dudhia, J. (1996), A multi-layer soil-temperature model for MM5, preprint, Sixth PSU/NCAR Mesoscale Model Users Workshop, Boulder, Colo.

Evans, J., R. Oglesby, and W. Lapenta (2005), Time series analysis of regional climate model performance, *J. Geophys. Res.*, *110*, D04104, doi:10.1029/2004JD005046.

Fernández, J. (2004), Statistical and dynamical downscaling models applied to winter precipitation on the Cantabrian coast, Ph.D. thesis, Univ. del País Vasco, Leioa, Spain.

Fernández, J., and J. Sáenz (2003), Improved field reconstruction with the analog method: Searching the CCA space, *Clim. Res.*, *24*, 199–213.

Fernández-Mills, G. (1995), Principal component analysis of precipitation and rainfall regionalization in Spain, *Theor. Appl. Climatol.*, *50*, 169–183.

Ferretti, R., T. Paolucci, W. Zheng, G. Visconti, and P. Bonelli (2000), Analyses of the precipitation pattern on the Alpine region using different cumulus convection parameterizations, *J. Appl. Meteorol.*, *39*, 182–200.

Font-Tullot, I. (2000), *Climatología de Espa na y Portugal*, 2nd ed., Ed. Univ. de Salamanca, Salamanca, Spain.

Giorgi, F., and L. O. Mearns (1999), Introduction to special section: Regional climate modeling revisited, *J. Geophys. Res.*, *104*(D6), 6335–6352.

Giorgi, F., and C. Shields (1999), Tests of precipitation parameterizations available in latest version of NCAR regional climate model (REGCM) over continental United States, *J. Geophys. Res.*, *104*(D6), 6353–6375.

González-Rouco, J. F., H. Heyen, E. Zorita, and F. Valero (2000), Agreement between observed rainfall trends and climate change simulations in the southwest of Europe, *J. Clim.*, *13*, 3057–3065.

González-Rouco, J. F., J. L. Jiménez, V. Quesada, and F. Valero (2001), Quality control and homogeneity of precipitation data in the southwest of Europe, *J. Clim.*, *14*, 964–978.

Goodess, C. M., and J. P. Palutikof (1998), Development of daily rainfall scenarios for southeast Spain using a circulation-type approach to downscaling, *Int. J. Climatol.*, *18*(10), 1051–1083.

Grell, G. A. (1993), Prognostic evaluation of assumptions used by cumulus parameterizations, *Mon. Weather Rev.*, *121*, 764–787.

Grell, G. A., J. Dudhia, and D. R. Stauffer (1994), A description of the fifth-generation Penn State/NCAR Mesoscale Model (MM5), *Tech. Rep. NCAR/TN-398+STR*, Natl. Cent. for Atmos. Res., Boulder, Colo.

Hewitson, B. C., and R. Crane (1996), Climate downscaling: Techniques and application, *Clim. Res.*, *7*, 85–95.

Hong, S. Y., and H. L. Pan (1996), Nonlocal boundary layer vertical diffusion in a medium-range forecast model, *Mon. Weather Rev.*, *124*, 2322–2339.

Janjić, Z. I. (1994), The step-mountain Eta coordinate model: Further developments of the convection, viscous sublayer, and turbulence closure schemes, *Mon. Weather Rev.*, *122*(5), 927–945.

Juang, H., and S. Hong (2001), Sensitivity of the NCEP regional spectral model to domain size and nesting strategy, *Mon. Weather Rev.*, *129*(12), 2904–2922.

Kain, J. S., and J. M. Fritsch (1990), A one-dimensional entraining/detraining plume model and its application in convective parameterization, *J. Atmos. Sci.*, *47*, 2784–2802.

Kalnay, E., et al. (1996), The NCEP/NCAR 40-year reanalysis project, *Bull. Am. Meteorol. Soc.*, *77*, 437–471.

Kidson, J. W., and C. S. Thompson (1998), A comparison of statistical and model-based downscaling techniques for estimating local climate variations, *J. Clim.*, *11*, 735–753.

Kotroni, V., and K. Lagouvardos (2001), Precipitation forecast skill of different convective microphysical schemes: Application for the cold season over Greece, *Geophys. Res. Lett.*, *28*, 1977–1980.

Leung, L., and S. Ghan (1999), Pacific northwest climate sensitivity simulated by a regional climate model driven by a GCM. Part I: Control simulations, *J. Clim.*, *12*(7), 2010–2030.

Leung, L., and M. Wigmosta (1999), Potential climate chance impacts on mountain watersheds in the Pacific northwest, *J. Am. Water Resour. Assoc.*, *35*(6), 1463–1471.

Leung, L., S. Zhong, Y. Qian, and Y. Liu (2004), Evaluation of regional climate simulations of the 1998 and 1999 east Asian summer monsoon using the GAME/HUBEX observational data, *J. Meteorol. Soc. Jpn.*, *82*(6), 1695–1713.

Liang, X., L. Li, A. Dai, and K. Kunkel (2004a), Regional climate model simulation of summer precipitation diurnal cycle over the United States, *Geophys. Res. Lett.*, *31*, L24208, doi:10.1029/2004GL021054.

Liang, X. Z., L. Li, K. E. Kunkel, M. Ting, and J. X. L. Wang (2004b), Regional climate model simulation of U.S. precipitation during 1982–2002. Part I: Annual cycle, *J. Clim.*, *17*, 3510–3529.

Lynn, B., L. Druyan, C. Hogrefe, A. Dudhia, C. Rosenzweig, R. Goldberg, D. Rind, R. Healy, J. Rosenthal, and P. Kinney (2004), Sensitivity of present and future surface temperatures to precipitation characteristics, *Clim. Res.*, *28*(1), 53–65.

Millán, M. M., B. Arti nano, L. Alonso, M. Navazo, and M. Castro (1991), The effect of meso-scale flows on regional and long-range atmospheric transport in the western Mediterranean area, *Atmos. Environ., Part A*, *25*, 949–963.

Mlawer, E. J., S. J. Taubman, P. D. Brown, M. J. Iacono, and S. A. Clough (1997), Radiative transfer for inhomogeneous atmospheres: RRTM, a validated correlated model for the longwave, *J. Geophys. Res.*, *102*, 16,663–16,682.

Moberg, A., and P. Jones (2004), Regional climate model simulations of daily maximum and minimum near-surface temperatures across europe compared with observed station data 1961–1990, *Clim. Dyn.*, *23*(7–8), 695–715.

Murphy, J. (1999), An evaluation of statistical and dynamical techniques for downscaling local climate, *J. Clim.*, *12*, 2256–2284.

New, M., M. Hulme, and P. Jones (1999), Representing twentieth-century space-time climate variability. Part I: Development of a 1961–90 mean monthly terrestrial climatology, *J. Clim.*, *12*(3), 829–856.

New, M., M. Hulme, and P. Jones (2000), Representing twentieth-century space-time climate variability. Part II: Development of 1901–96 monthly grids of terrestrial surface climate, *J. Clim.*, *13*, 2217–2238.

Noguer, M., R. Jones, and J. Murphy (1998), Sources of systematic errors in the climatology of a regional climate model over Europe, *Clim. Dyn.*, *14*(10), 691–712.

Oh, J., T. Kim, M. Kim, S. Lee, S. Min, and W. Kwon (2004), Regional climate simulation for Korea using dynamic downscaling and statistical adjustment, *J. Meteorol. Soc. Jpn.*, *82*(6), 1629–1643.

Oñate, J. J., and A. Pou (1996), Temperature variations in Spain since 1901: A preliminary analysis, *Int. J. Climatol.*, *16*, 805–815.

Pan, Z., E. Takle, M. Segal, and R. Turner (1996), Influences of model parameterization schemes on the response of rainfall to soil moisture in the central United States, *Mon. Weather Rev.*, *124*, 1786–1802.

Paredes, D., R. M. Trigo, R. García-Herrera, and I. F. Trigo (2006), Understanding precipitation changes in Iberia in early spring: Weather typing and storm-tracking approaches, *J. Hydrometeorol.*, *7*, 101–113.

Pielke, R. (2001), Influence of the spatial distribution of vegetation and soils on the prediction of cumulus convective rainfall, *Rev. Geophys.*, *39*(2), 151–177.

Pozo-Vázquez, D., M. J. Esteban-Parra, F. S. Rodrigo, and Y. Castro-Díez (2001), A study of NAO variability and its possible non-linear influences on European surface temperature, *Clim. Dyn.*, *17*, 701–715.

Reisner, J., R. M. Rasmussen, and R. T. Bruintjes (1998), Explicit forecasting of supercooled liquid water in winter storms using the MM5 mesoscale model, *Q. J. R. Meteorol. Soc.*, *124*, 1071–1107.

Rodó, X., E. Baert, and F. A. Comin (1997), Variations in seasonal rainfall in southern Europe during the present century: Relationships with the North Atlantic Oscillation and the El Ni\ no–Southern Oscillation, *Clim. Dyn.*, *13*, 275–284.

Rodríguez-Fonseca, B., and E. Serrano (2002), Winter 10-day coupled patterns between geopotential height and Iberian Peninsula rainfall using the ECMWF precipitation reanalysis, *J. Clim.*, *15*(11), 1309–1321.

Rodríguez-Puebla, C., A. H. Encinas, S. Nieto, and J. Garmendia (1998), Spatial and temporal patterns of annual precipitation variability over the Iberian Peninsula, *Int. J. Climatol.*, *18*, 299–316.

Rodríguez-Puebla, C., A. H. Encinas, and J. Sáenz (2001), Winter precipitation over the Iberian Peninsula and its relationship to circulation indices, *Hydrol. Earth Syst. Sci.*, *5*(2), 233–244.

Romero, R., C. Ramis, and J. A. Guijarro (1999), Daily rainfall patterns in the Spanish Mediterranean area: An objective classification, *Int. J. Climatol.*, *19*(1), 95–112.

Sáenz, J., C. Rodríguez-Puebla, J. Fernández, and J. Zubillaga (2001a), Interpretation of interannual winter temperature variations over southwestern Europe, *J. Geophys. Res.*, *106*(D18), 20,641–20,652.

Sáenz, J., J. Zubillaga, and C. Rodríguez-Puebla (2001b), Interannual winter temperature variability in the north of the Iberian Peninsula, *Clim. Res.*, *16*(3), 169–179.

Sáenz, J., J. Zubillaga, and C. Rodríguez-Puebla (2001c), Interannual variability of winter precipitation in northern Iberian Peninsula, *Int. J. Climatol.*, *21*(12), 1503–1513.

Salvador, R., J. Calbo, and M. Millan (1999), Horizontal grid size selection and its influence on mesoscale model simulations, *J. Appl. Meteorol.*, *38*(9), 1311–1329.

Serrano, A., J. E. García, V. L. Mateos, M. L. Cancillo, and J. Garrido (1999), Monthly modes of variation of precipitation over the Iberian Peninsula, *J. Clim.*, *12*, 2894–2919.

Sumner, G. N., R. Romero, V. Homar, C. Ramis, S. Alonso, and E. Zorita (1995), An estimate of the effects of climate change on the rainfall of Mediterranean Spain by the late twenty first century, *Int. J. Climatol.*, *15*, 673–696.

Trigo, R., and J. Palutikof (1999), Simulation of daily temperatures for climate change scenarios over Portugal: A neural network model approach, *Clim. Res.*, *13*(1), 45–59.

Trigo, R. M., and J. P. Palutikof (2001), Precipitation scenarios over Iberia: A comparison between direct GCM output and different downscaling techniques, *J. Clim.*, *14*, 4422–4446.

Ulbrich, U., M. Christoph, J. G. Pinto, and J. Corte-Real (1999), Dependence of winter precipitation over Portugal on NAO and baroclinic wave activity, *Int. J. Climatol.*, *19*, 379–390.

Uppala, S., et al. (2005), The ERA-40 re-analysis, *Q. J. R. Meteorol. Soc.*, *131*, 2961–3012.

Vidale, P. L., D. Lüthi, C. Frei, S. I. Seneviratne, and C. Schär (2003), Predictability and uncertainty in a regional climate model, *J. Geophys. Res.*, *108*(D18), 4586, doi:10.1029/2002JD002810.

von Storch, H., E. Zorita, and U. Cubasch (1993), Downscaling of global climate change estimates to regional scales: An application to Iberian rainfall in wintertime, *J. Clim.*, *6*, 1161–1171.

Wang, P., and J. Yang (2003), Observation and numerical simulation of cloud physical processes associated with torrential rain of the Meiyu front, *Adv. Atmos. Sci.*, *20*(1), 77–96.

Wang, W., and N. L. Seaman (1997), A comparison study of convective parameterization schemes in a mesoscale model, *Mon. Weather Rev.*, *125*, 252–278.

Wang, Y., L. Leung, J. McGregor, D. Lee, W. Wang, Y. Ding, and F. Kimura (2004), Regional climate modeling: Progress, challenges, and prospects, *J. Meteorol. Soc. Jpn.*, *82*(6), 1599–1628.

Warner, T. T., and H. Hsu (2000), Nested-model simulation of moist convection: The impact of coarse-grid parameterized convection on fine-grid resolved convection, *Mon. Weather Rev.*, *128*, 2211–2231.

Warner, T., R. Peterson, and R. Treadon (1997), A tutorial on lateral boundary conditions as a basic and potentially serious limitation to regional numerical weather prediction, *Bull. Am. Meteorol. Soc.*, *78*(11), 2599–2617.

Wessel, P., and W. H. F. Smith (1991), Free software helps map and display data, *Eos Trans. AGU*, *72*, 441.

Wisse, J., and J. Vilá-Guerau (2004), Analysis of the role of the planetary boundary layer schemes during a severe convective storm, *Ann. Geophys.*, *22*(6), 1861–1874.

Worley, S., S. Woodruff, R. Reynolds, S. Lubker, and N. Lott (2005), ICOADS release 2.1 data and products, *Int. J. Climatol.*, *25*(7), 823–842.

Wu, W., A. Lynch, and A. Rivers (2005), Estimating the uncertainty in a regional climate model related to initial and lateral boundary conditions, *J. Clim.*, *18*(7), 917–933.

Xie, P., and P. A. Arkin (1997), Global precipitation: A 17-year monthly analysis based on gauge observations, satellite estimates, and numerical model outputs., *Bull. Am. Meteorol. Soc.*, *78*, 2539–2558.

Xoplaki, E., J. F. González-Rouco, J. Luterbacher, and H. Wanner (2003), Mediterranean summer air temperature variability and its connection to the large-scale atmospheric circulation and SSTs, *Clim. Dyn.*, *20*, 723–739.

Xoplaki, E., J. Gonzalez-Rouco, J. Luterbacher, and H. Wanner (2004), Wet season mediterranean precipitation variability: Influence of large-scale dynamics and trends, *Clim. Dyn.*, *23*(1), 63–78.

Zhang, D., and R. A. Anthes (1982), A high-resolution model of the planetary boundary layer-sensitivity tests and comparisons with SESAME-79 data, *J. Appl. Meteorol.*, *21*, 1594–1609.

Zhu, J., and X.-Z. Liang (2005), Regional climate model simulation of U.S. soil temperature and moisture during 1982–2002, *J. Geophys. Res.*, *110*, D24110, doi:10.1029/2005JD006472.

J. Fernández and E. Zorita, Institute for Coastal Research, GKSS Forschungszentrum, Max-Planck-Str. 1, D-21502 Geesthacht, Germany. (fernandej@unican.es; zorita@gkss.de)

J. F. González-Rouco, Departamento de Astrofísica y CC. de la Atmósfera, Universidad Complutense de Madrid, E-28040 Madrid, Spain. (fidelgr@fis.ucm.es)

J. P. Montávez, Departamento de Física, University of Murcia, Campus de Espinardo, E-30071 Murcia, Spain. (montavez@um.es)

J. Sáenz, Department of Applied Physics II, University of the Basque Country, Apdo. 644, E-48080 Bilbao, Spain. (jon.saenz@ehu.es)